HNUE JOURNAL OF SCIENCE
Journal of Natural Sciences, 2026, Volume 71, Issue 2, pp. 34-44
This paper is available online at http://hnuejs.edu.vn/ns
DOI: 10.18173/2354-1059.2026-0018

# ELECTRONIC PHASES OF THE IONIC HUBBARD MODEL WITH COULOMB DISORDER

Nguyen Thi Hai Yen[1,*], Hoang Anh Tuan[1] and Le Duc Anh[2]
[1]*Institute of Physics, Vietnam Academy of Science and Technology, Hanoi, Vietnam*
[2]*Hanoi National University of Education, Hanoi, Vietnam*
*Corresponding author: Nguyen Thi Hai Yen, e-mail: nhyen@iop.vast.vn

Received January 26, 2026. Revised April 24, 2026. Accepted June 30, 2026.

**Abstract.** We investigate the effects of Coulomb disorder on the half-filled ionic Hubbard model within the framework of dynamical mean-field theory (DMFT), using the equation-of-motion method as the impurity solver, combined with typical medium theory (TMT). In contrast to conventional disordered Hubbard models, the ionic Hubbard model contains a staggered ionic potential that introduces additional competition between band-insulating and correlation-driven insulating tendencies. We analyze how this ionic potential modifies the electronic phases induced by Coulomb disorder through the arithmetic and geometric averages of the local density of states. In the absence of disorder, the system exhibits metallic (M), Mott-insulating (MI), and band-insulating (BI) phases. When Coulomb disorder is introduced, Anderson-insulating (AI) behavior and localized states (LS) inside the Mott gap are also observed. In particular, the LS regime appears between the metallic and Mott-insulating phases at small ionic potentials, whereas the AI regime develops for sufficiently large values of the Coulomb interaction and ionic potential. Our results show that the interplay between ionic potential, electron correlation, and disorder substantially influences the localization behavior and insulating characteristics of the ionic Hubbard model.
***Keywords:*** Metal–insulator transitions, ionic Hubbard model, Coulomb disorder.

## 1. Introduction

Metal–insulator transitions (MITs) are a fundamental topic in condensed matter physics. Strong electron–electron correlations can drive a Mott transition [1], whereas disorder can induce Anderson localization [2]. Understanding the interplay between correlation and disorder remains one of the central problems in strongly correlated systems . The ionic Hubbard model (IHM) [3]-[7] is an extension of the Hubbard model originally proposed to study the neutral–ionic transition in organic charge-transfer salts

or the ferroelectric transition in perovskite materials. In addition to the on-site Coulomb interaction $U$, the model contains a staggered ionic potential ($\pm\Delta$) on a bipartite lattice, where the two sublattices ($A$ and $B$) have on-site energy levels differing by $2\Delta$. The presence of this ionic potential breaks the equivalence between the two sublattices and induces charge disproportionation, leading to insulating behavior.

In general, the effects of disorder and Coulomb interaction are commonly studied in conventional Hubbard-type models such as the Anderson–Hubbard model (AHM) [8], [9] and the Anderson–Falicov–Kimball model (AFKM) [10]-[13]. While Anderson localization and disorder-induced insulating behavior have been extensively investigated in these systems, the role of a staggered ionic potential in modifying such effects remains less explored. In the ionic Hubbard model, the coexistence of band-insulating tendencies, electron correlation, and disorder leads to a richer competition among different localization mechanisms. Therefore, this work aims to identify and characterize the resulting disorder-induced electronic phases within the ionic Hubbard framework.

In realistic materials, Coulomb disorder naturally arises from spatial inhomogeneities in the charge distribution, background doping, and unintentional charged impurities [14]. For this reason, investigating the effects of Coulomb disorder is important for understanding realistic strongly correlated systems.

Dynamical mean-field theory (DMFT) [15] is one of the most powerful methods for investigating strongly correlated electron systems. Within DMFT, the many-body problem is mapped onto an effective single-impurity problem embedded in a noninteracting bath. Several impurity solvers have been developed, including quantum Monte Carlo (QMC) [15], numerical renormalization group (NRG) [16], exact diagonalization (ED) [17], and equation-of-motion (EOM) approaches. In this work, we employ the EOM method as the impurity solver. Although the EOM approach depends on the truncation scheme used for the hierarchy of equations of motion, it works directly on the real-frequency axis, is computationally efficient, and is suitable for low-temperature calculations. Thus, it is appropriate for obtaining qualitative insights into the interplay among electron correlation, ionic potential, and disorder in the present model.

The arithmetic average of the local density of states (LDOS) can describe the gap opening at the Fermi level associated with the Mott transition. However, it generally remains finite even in the Anderson-insulating phase and therefore cannot properly capture Anderson localization. To overcome this limitation, typical medium theory (TMT) [18] employs the geometric average of the LDOS as an effective order parameter for the Anderson transition. Consequently, combining the arithmetic and geometric averages allows one to distinguish metallic, Mott-insulating, and Anderson-insulating phases.

In this work, we investigate the competing phases of the disordered ionic Hubbard model within the framework of DMFT using the EOM method as the impurity solver. The phases are characterized through the arithmetic and geometric averages of the LDOS,

with emphasis on qualitative phase identification rather than quantitatively precise critical boundaries. The remainder of this paper is organized as follows. Section 2 and 3 presents the model, theoretical methods, and numerical results, while Section 4 summarizes the main conclusions.

## 2. Model and methods

The Hamiltonian of the IHM with Coulomb disorder is given as follows:

$$H = -t \sum_{i\in A, j\in B, <ij>\sigma} \left( c^{\dagger}_{i\sigma} c_{j\sigma} + H.c. \right) + \varepsilon_A \sum_{i\in A\sigma} n_{i\sigma} + \varepsilon_B \sum_{i\in B\sigma} n_{i\sigma} + \sum_i U_i n_{i\uparrow} n_{i\downarrow}, \tag{2.1}$$

where $c_{i\sigma}(c^{\dagger}_{i\sigma})$ annihilates (creates) an electron with spin $\sigma$ at site $i$, $n_{i\sigma} = c^{\dagger}_{i\sigma} c_{i\sigma}$, and the sum $< i, j >$ is over nearest-neighbor sites. $\varepsilon_A = \Delta$, $\varepsilon_B = -\Delta$ are the ionic energies, and $\Delta$ is chosen to be positive. $t$ denotes the nearest-neighbor hopping integral. $U_i$ is the on-site Coulomb repulsion and is a random variable following a box probability distribution

$$P(U_i) = \frac{1}{\delta} \Theta \left( \frac{\delta}{2} - |U_i - U| \right). \tag{2.2}$$

$U$ is the mean value of the Coulomb interaction, and $\delta$ is the disorder strength. Here, we consider only the repulsive interaction, meaning $U_i \geq 0$, from which $U \geq \delta/2$. Within the DMFT framework, the many-particle problem is mapped onto a single impurity embedded in a bath of noninteracting electrons. In the paramagnetic case, the spin index is omitted for simplicity. The local Green's function $G_\alpha(\omega, U_i)$ ($\alpha = A, B$) corresponding to Eq. (1) is given by

$$\begin{aligned} G_\alpha(U_i, \omega) = & \frac{1 - \langle n_\alpha \rangle/2}{G^{-1}_{0\alpha} + U_i \Pi_{1\alpha}(\omega) \left[ G^{-1}_{0\alpha} - U_i - \Pi_{3\alpha}(\omega) \right]^{-1}} \\ & + \frac{\langle n_\alpha \rangle/2}{G^{-1}_{0\alpha} - U_i - U_i \Pi_{2\alpha}(\omega) \left[ G^{-1}_{0\alpha} - \Pi_{3\alpha}(\omega) \right]^{-1}}, \end{aligned} \tag{2.3}$$

where the bare Green's function of the associated quantum impurity problem for sublattice $\alpha$ is $G_{0\alpha} = [\omega - \varepsilon_\alpha + U_i/2 - \eta_\alpha(\omega)]^{-1}$. The impurity electron interacts with the noninteracting electrons through a hybridization function $\eta_\alpha(\omega)$.

The self-energies $\Pi_{1\alpha}(\omega)$, $\Pi_{2\alpha}(\omega)$, and $\Pi_{3\alpha}(\omega)$ can be expressed through the hybridization function as follows:

$$\Pi_{k\alpha}(\omega) = \int_{-\infty}^{+\infty} \eta_\alpha(z) F_k(z) \left( \frac{1}{\omega - z} + \frac{1}{\omega - 2\epsilon_\alpha + z} \right) dz, \tag{2.4}$$

where $k = 1, 2, 3$. $F_1(z) = f(z) = \dfrac{1}{1 + \exp(z/T)}$ is the Fermi function, $F_2(z) = 1 - F_1(z)$, and $F_3(z) = 1$.

For a bipartite lattice, the Green's function for each sublattice is given by

$$G_\alpha(\omega) = G_{ii\alpha}(\omega) = \int_{-\infty}^{\infty} \frac{\xi_{\overline{\alpha}}(\omega)\rho^0(z)dz}{\xi_A(\omega)\xi_B(\omega) - z^2}, \tag{2.5}$$

where $\alpha = A, B$ and $\overline{\alpha} = B, A$, respectively, and $\xi_\alpha = \omega + \mu_\alpha - \Sigma_\alpha(\omega)$, with $\mu_\alpha = \mu - \varepsilon_\alpha$; $\Sigma_\alpha$ is the local self-energy for sublattice $\alpha$, and $\rho^0(z)$ is the noninteracting density of states (DOS). For the Bethe lattice with infinite coordination number,

$$\rho^0(z) = \frac{1}{2\pi t^2}\sqrt{4t^2 - z^2}. \tag{2.6}$$

By substituting the Bethe-lattice DOS from Eq. (2.6) into Eq. (2.5), we obtain the self-consistency condition:

$$\eta_\alpha(\omega) = \frac{W^2}{16} G_{\overline{\alpha}}(\omega), \tag{2.7}$$

where $\alpha = A, B$ and $\overline{\alpha} = B, A$, respectively, and the bandwidth is $W = 4t$. In the bipartite lattice, the hybridization function on sublattice *A* is related to the local Green's function of sublattice *B* due to the hopping between the two sublattices. Therefore, the electronic properties of the two sublattices are mutually dependent.

In this paper, we consider the paramagnetic, half-filled case, i.e., $< n_{\alpha\uparrow} >=< n_{\alpha\downarrow} >=< n_\alpha > /2$ and $\mu = 0$.

The LDOS is given by

$$\rho_\alpha(\omega, U_i) = -\frac{1}{\pi}\mathrm{Im}G_\alpha(\omega, U_i), \;\; \alpha = \{A, B\}. \tag{2.8}$$

The geometric and arithmetic averages of the LDOS are

$$\rho_{\alpha,geom}(\omega) = \exp\langle \ln \rho(\omega, U_i)\rangle, \tag{2.9}$$

$$\rho_{\alpha,arith}(\omega) = \langle \rho(\omega, U_i)\rangle\,, \tag{2.10}$$

where $\langle O(U_i)\rangle = \int dU_i P(U_i) O(U_i)$. Equations (2.5) and (2.7) constitute the self-consistency equations for $G_\alpha(\omega)$ ($\alpha = A, B$). These equations must be solved with the condition $n_A + n_B = 2$, where $n_\alpha = -\frac{1}{\pi}\int_{-\infty}^{0} d\omega \Im G_{\alpha,arith}(\omega)$. It should be noted that the average particle number on sublattices $A$ and $B$ is calculated using the arithmetically averaged Green's function, since the geometric average describes only extended states, whereas the arithmetic average accounts for both localized and extended states.

## 3. Results and discussion

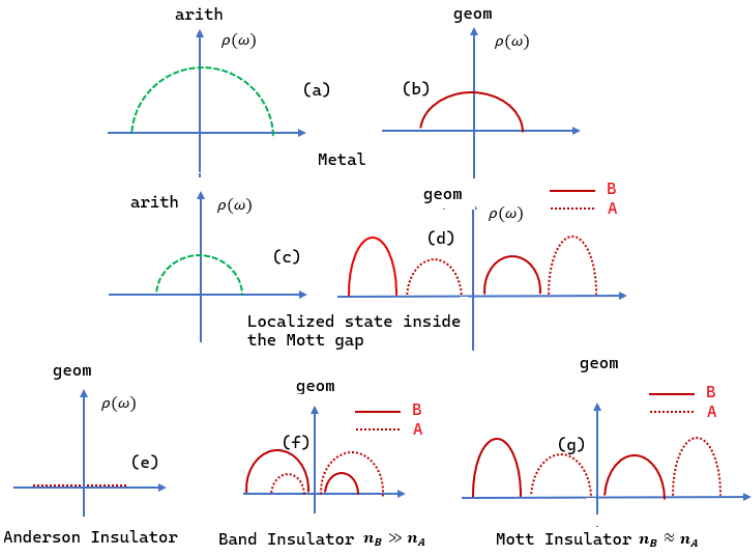


***Figure 1. Schematic illustration of phase definitions in the ionic Hubbard model based on the arithmetic (green lines) and geometric (red lines) averages of the LDOS. Panels (a, b) correspond to the metallic phase, (c, d) to localized states within the Mott gap, (e) the Anderson insulator, (f) the band insulator, and (g) the Mott insulator.***

We use the bandwidth as the unit of energy. We investigate the electronic phases of the system using the equation-of-motion (EOM) method to solve the impurity problem. The state of the system is determined by the geometric and arithmetic averages of the LDOS $\rho_{\alpha,geom}(\omega)$, $\rho_{\alpha,arith}(\omega)$ together with the behavior of the staggered charge density $n_B - n_A$ (ionicity). For all finite ionic potentials $\Delta > 0$, electrons tend to occupy the lower-energy sites of sublattice $B$, leading to $n_B > n_A$. Therefore, the ionicity $n_B - n_A$ cannot be regarded as a true order parameter. Nevertheless, it serves as an indicator distinguishing the two insulating phases: it tends to zero in the Mott-insulating phase, whereas $n_B \gg n_A$ in the band-insulating phase.

The electronic states are classified as follows (see Figure 1): Metal (M): $\rho_{\alpha a}(0) \neq 0, \rho_{\alpha g}(0) \neq 0$; band insulator (BI): $\rho_{\alpha a}(0) = 0, \rho_{\alpha g}(0) = 0, \int \rho_{\alpha g}(\omega)d\omega \neq 0$, $n_B \gg n_A$; localized states (LS) inside the Mott gap: $\rho_{\alpha a}(0) \neq 0, \rho_{\alpha g}(0) = 0, \int \rho_{\alpha g}(\omega)d\omega \neq 0$; Mott insulator: $\rho_{\alpha a}(0) = 0, \rho_{\alpha g}(0) = 0, \int \rho_{\alpha g}(\omega)d\omega \neq 0$, $n_B \approx n_A$; Anderson insulator (AI): $\int \rho_{\alpha g}(\omega)d\omega = 0$.

To illustrate this more clearly, we present Figure 2, which shows the DOS in the Anderson-localized regime. In the regime of strong $U$ and intermediate to large $\Delta$, the geometric average of the LDOS vanishes over the entire frequency range, whereas the arithmetic average remains finite. This behavior characterizes an Anderson-insulating regime and indicates that disorder strongly suppresses the extended electronic states.

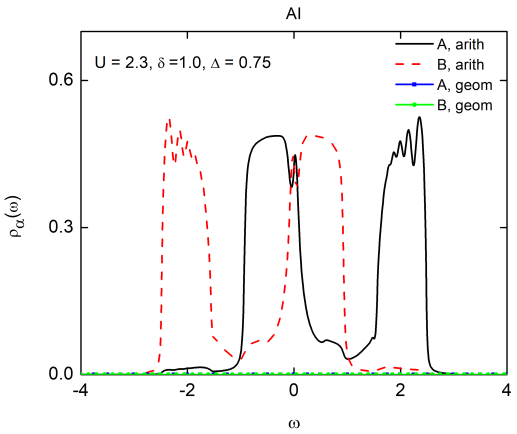


***Figure 2. Arithmetic (solid and dashed lines) and geometric (square and circle symbols) averages of the LDOS for sublattices A and B in the Anderson-insulating (AI) phase.***

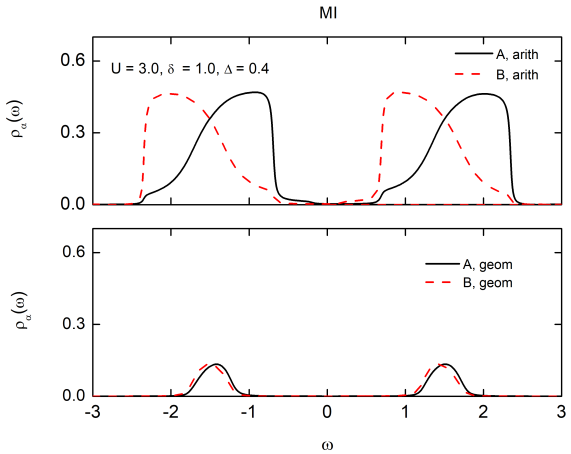


***Figure 3. The upper panel shows the arithmetic average of the LDOS, while the lower panel shows the geometric average. Solid and dashed lines correspond to sublattices $A$ and $B$, respectively. The system is in the Mott-insulating phase (MI).***

To further clarify the influence of Coulomb disorder, we present in Figure 3 the density of states (DOS) of the Mott-insulating phase at a finite Coulomb disorder strength ($\delta \neq 0$) and large $U$, obtained from both the arithmetic and geometric averages of the LDOS. In this phase, the ionicity $n_B - n_A$ gradually approaches zero near the critical point. As the disorder strength increases, the Anderson-insulating (AI) regime expands in parameter space, leading to a reduction in the stability region of the Mott insulator compared to the disorder-free case. This behavior indicates that the MI phase is progressively suppressed due to the enhanced tendency toward Anderson localization.

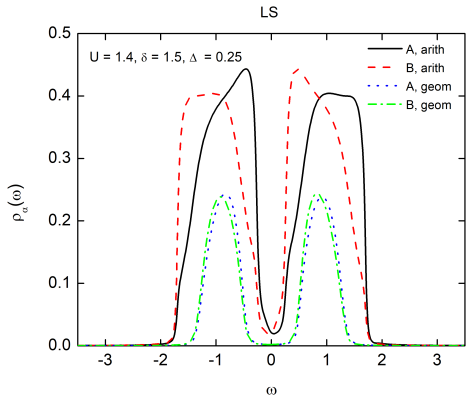


***Figure 4. Arithmetic (solid and dashed) and geometric (dotted and dash-dotted) averages of the LDOS for sublattices A and B in the localized-states (LS) regime within the Mott gap.***

In Figure 4, we illustrate the emergence of localized states (LS) within the Mott-gap regime. In this case, the LDOS at the Fermi level vanishes in the geometric average, while it remains finite in the arithmetic average. These results are consistent with those obtained for the ionic Hubbard model with Coulomb disorder ($\Delta = 0$) [19]. We further find that the LS solution appears in a narrow regime between the metallic and Mott-insulating phases at small values of $U$ and $\Delta$. The LS regime can thus be viewed as an intermediate state between extended (metallic) and localized (insulating) phases.

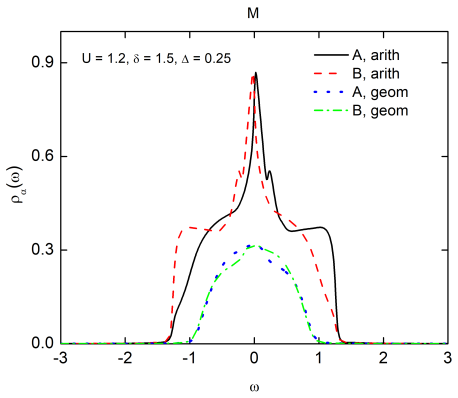


***Figure 5. Same as in Figure 4, but for the metallic phase (M).***

In the metallic phase (Figure 5), both the arithmetic and geometric averages of the LDOS remain finite at the Fermi level, indicating the presence of extended electronic states. As disorder is introduced and gradually increased, the metallic regime slightly expands around the critical points of the clean system. This originates from the spatial randomness of the local Coulomb interaction $U_i$ at different lattice sites, where some

lattice sites satisfy $U_i < U$, which locally suppresses correlation effects and enhances electron mobility. By contrast, under strong disorder, the metallic regime is reduced due to the dominance of the Anderson-insulating phase.

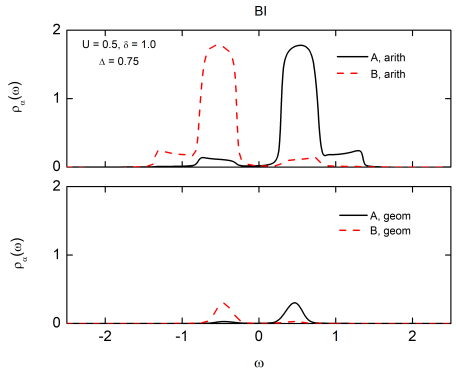


***Figure 6. Same as in Figure 3, but for the band insulating phase (BI).***

In the absence of disorder ($\delta = 0$), the ionic potential stabilizes the band-insulating (BI) phase, which already emerges at finite values of $\Delta$ [4]. However, upon introducing disorder, the BI (Figure 6) regime with $n_B \gg n_A$ progressively shrinks and becomes confined to the large-$\Delta$ regime before eventually disappearing at stronger disorder, mainly due to the expansion of the metallic and Anderson-insulating phases.

Finally, to emphasize disorder-induced solutions, in Figure 7 we present the emergence of the LS solution between the M and MI phases. In the presence of Coulomb disorder, at a fixed ionic potential $\Delta$, increasing the Coulomb interaction drives the system through an intermediate LS regime that separates the metallic (M) and Mott-insulating (MI) phases. In addition, Figure 8 shows the transition from the M phase to the AI phase as the Coulomb interaction increases at fixed disorder $\delta$ and ionic potential $\Delta$.

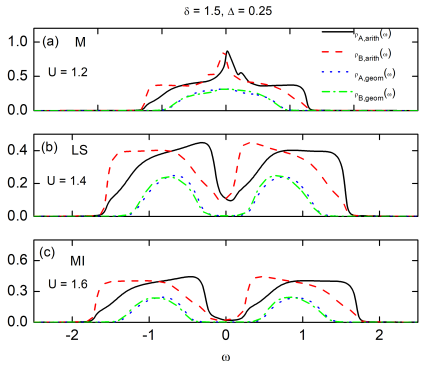


***Figure 7. Emergence of localized states inside the Mott gap (LS) regime between the metallic (M) and Mott-insulating (MI) phases as $U$ increases from (a) to (c) at fixed $\delta$ in the small $\Delta$ regime.***

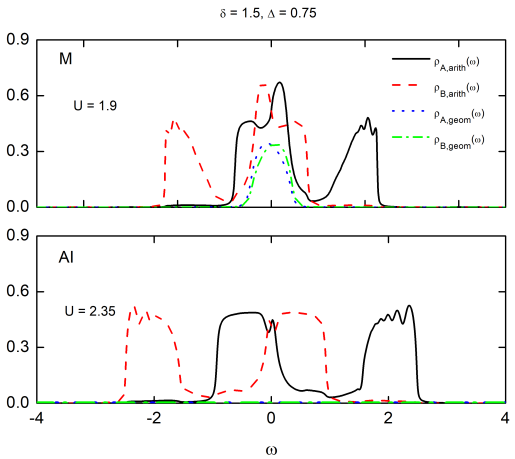


***Figure 8. Evolution from the metallic (M) phase to the Anderson-insulating (AI) phase as $U$ increases from (a) to (b) at fixed $\Delta$ and $\delta$.***

## 4. Conclusions

In conclusion, using the EOM as the impurity solver within DMFT, we investigated the effects of Coulomb disorder on the ionic Hubbard model. We showed that the staggered ionic potential plays an important role in determining the electronic phases of the system. In the disorder-free case, the ionic potential stabilizes the conventional metallic (M), Mott-insulating (MI), and band-insulating (BI) phases. Upon introducing Coulomb disorder, additional electronic solutions emerge, including the Anderson-insulating (AI) phase and a localized-states (LS) regime inside the Mott gap. In particular, the LS regime appears between the metallic and Mott-insulating phases in the small-$\Delta$ region, whereas the AI phase becomes dominant at sufficiently large values of the Coulomb interaction and ionic potential. Furthermore, weak disorder slightly expands the metallic regime around the critical regions of the disorder-free system. However, at stronger disorder, the Anderson-insulating phase becomes dominant, leading to the suppression of metallic behavior as well as the progressive reduction of the BI and MI phases.

The present work focuses on the characterization of representative electronic phases and localization regimes in the disordered ionic Hubbard model. A systematic determination of the full phase boundaries and critical behavior throughout the $(U, \Delta, \delta)$ parameter space remains an interesting direction for future investigation.

***Note for contributor***:

- Short bio: Nguyen Thi Hai Yen is a researcher at the Institute of Physics, Vietnam Academy of Science and Technology, Vietnam; Hoang Anh Tuan is a researcher at the Institute of Physics, Vietnam Academy of Science and Technology, Vietnam; and Le Duc Anh is a lecturer at Hanoi National University of Education, Vietnam.

- Author's contributions: Nguyen Thi Hai Yen: conceptualization, methodology,

investigation, formal analysis, writing-original draft; Hoang Anh Tuan: formal analysis, discussion, writing; and Le Duc Anh: review, discussion, writing, and editing.

***Conflict of interest***. The authors declare no conflict of interest.

***Acknowledgments***. This work was supported by the International Centre of Physics at the Institute of Physics, Vietnam Academy of Science and Technology under Grant ICP.2024.12.

## REFERENCES

[1] N. F. Mott, "Electrons in disordered structures", *Advances in Physics*, vol. 16, no. 61, pp. 49–144, 1967. http://dx.doi.org/10.1080/00018736700101265

[2] P. W. Anderson, "Absence of diffusion in certain random lattices", *Physical Review*, vol. 109, no. 5, pp. 1492–1505, 1958. DOI: https://doi.org/10.1103/PhysRev.109.1492

[3] J. Hubbard and J. B. Torrance, "Model of the Neutral-Ionic Phase Transformation", *Physical Review Letters*, vol. 47, no. 54, pp. 1747–1750, 1981. DOI: https://doi.org/10.1103/PhysRevLett.47.1750

[4] H. A. Tuan, "Metal–insulator transitions in the half-filled ionic Hubbard model", *Journal of Physics: Condensed Matter* vol. 22, no. 9, p 095602, 2010. DOI: 10.1088/0953-8984/22/9/095602

[5] X. Zhuotao, et al., "Quench dynamics in the one-dimensional mass-imbalanced ionic Hubbard model", *Physical Review B*, vol. 107, no. 9, p 195147, 2023. DOI: https://doi.org/10.1103/PhysRevB.107.195147

[6] O. A. Moreno Segura, K. Hallberg, A. A. Aligia, "Charge and spin gaps in the ionic Hubbard model with density-dependent hopping", *Physical Review B*, vol. 108, no. 19, p 195135, 2023. DOI: https://doi.org/10.1103/PhysRevB.108.195135

[7] N. T. H. Yen & H. A. Tuan, "Metal-insulator transitions in the two-dimensional ionic Hubbard model within coherent potential approximation", *Communications in Physics*, vol. 36, no. 1, pp 19-26, 2026. DOI: https://doi.org/10.15625/0868-3166/23350

[8] K. Byczuk, W. Hofstetter, D. Vollhardt, "Anderson localization vs. Mott Hubbard metal-insulator transition in disordered, interacting lattice fermion systems", *International Journal of Modern Physics B*, vol. 24, no. 12n13, pp. 1727–1755, 2010. DOI: 10.1142/S0217979210064575

[9] M. C. O. Aguiar, V. Dobrosavljevic, E. Abrahams, G. Kotliar, "Critical Behavior at the Mott-Anderson Transition: A Typical-Medium Theory Perspective", *Physical Review Letters*, vol. 102, no. 15, p 156402, 2009. DOI: https://doi.org/10.1103/PhysRevLett.102.156402

[10] K. Byczuk, et al., "Mott-Hubbard Transition versus Anderson Localization in Correlated Electron Systems with Disorder", *Physical Review Letters*, vol. 94, no. 5, p 056404, 2005. DOI: https://doi.org/10.1103/PhysRevLett.94.056404

[11] R. D. B. Carvalho, M. A. Gusmao, “Effects of band filling in the Anderson-Falicov-Kimball model”, *Physical Review B*, vol. 87, no. 8, p 085122, 2013. DOI: https://doi.org/10.1103/PhysRevB.87.085122

[12] J. Park and E. Khatami, “Thermodynamics of the disordered Hubbard model studied via numerical linked-cluster expansions”, *Physical Review B*, vol. 104, no. 16, p 165102, 2021. DOI: https://doi.org/10.1103/PhysRevB.104.165102

[13] W. Morong et al., “Disorder-controlled relaxation in a three-dimensional Hubbard model quantum simulator”, *Physical Review Research*, vol. 3, no. 1, L012009, 2021. DOI: https://doi.org/10.1103/PhysRevResearch.3.L012009

[14] K. W. Kim et al., “Metal-insulator transition in a disordered and correlated SrTi1-xRuxO3 system: Changes in transport properties, optical spectra, and electronic structure”, *Physical Review B*, vol. 71, no. 12, p 125104, 2005. DOI: https://doi.org/10.1103/PhysRevB.71.125104

[15] A. Georges, G. Kotliar, W. Krauth and M. J. Rosenberg, “Dynamical mean-field theory of strongly correlated fermion systems and the limit of infinite dimensions”, *Reviews of Modern Physics*, vol. 68, no. 1, pp 13-125, 1996. DOI: https://doi.org/10.1103/RevModPhys.68.13

[16] R. Bulla, A. C. Hewson and Th. Pruschke, “Numerical renormalization group calculations for the self-energy of the impurity Anderson model”, *Journal of Physics: Condensed Matter*, vol. 10, no. 37, pp. 8365–8380, 1998. DOI: 10.1088/0953-8984/10/37/021

[17] Y. Lu, M. W. Haverkort, “Exact diagonalization as an impurity solver in dynamical mean field theory”, *The European Physical Journal Special Topics*, vol. 226, no. 11-12, pp 2549–2564, 2017. https://doi.org/10.1140/epjst/e2017-70042-4

[18] V. Dobrosavljevic et al., “Typical medium theory of Anderson localization: A local order parameter approach to strong-disorder effects”, *Europhysics Letters*, vol. 62, no. 1, pp. 76–82, 2003. DOI: 10.1209/epl/i2003-00364-5

[19] N. T. H. Yen, L. D. Anh & H. A. Tuan, “Anderson localization in the Anderson–Hubbard model with site-dependent interactions”, *New Journal of Physics*, vol. 24, no. 5, p 053054, 2022. DOI: 10.1088/1367-2630/ac706e